CCIT Report #425 May 2003

Amplitude Modulated Multipulse PPM for Bandwidth-Limited Optical Systems

Bassel Haddad * Shraga I. Bross †

May 22, 2003

Abstract

Optical direct-detection systems have been considered before for high-speed intersatellite links. In this paper we consider a three-level amplitude modulated multipulse PPM for use in bandwidth limited optical systems. Specifically, we investigate the capacity, cutoff rate, and error probability of this modulation scheme. This facilitates the evaluation of the bandwidth efficiency of the proposed modulation as compared to regular multipulse PPM which delivers the same throughput and detection quality under the same average-power constraint.

Index Terms – Optical systems, error probability, modulation, bandwidth efficiency.

*Zoran Microelectronics, Haifa 31024, Israel email:basselh@zoran.co.il
†Department of Electrical Engineering Technion, Haifa 32000, Israel email:shraga@ee.technion.ac.il

I. Introduction

Optical direct detection systems have long been considered for deep-space communication. For moderate data rates and where good performance for low-power consumption is paramount; pulse-position modulation (PPM) was shown to be a suitable modulation scheme [1, 2]. When higher data rates are considered PPM seems to exhibit inherent throughput limitation since the only way throughput can increase is by reducing the pulsewidth. This is unacceptable when the transmitter is subject to stringent bandwidth constraint. In order to improve the transmission efficiency under a given bandwidth constraint, two alternative techniques have been suggested. The first scheme is overlapping PPM (OPPM), wherein more than one pulse-position per pulsewidth is allowed in order to maintain low duty-cycle, yet while preserving some of the desirable properties of PPM. This scheme was originally studied in [3] and later in [4, 5, 6, 8].

Another modulation scheme that has been considered recently in the literature is multipulse or combinatorial PPM (MPPM) [9, 10, 7]. This modulation scheme is a generalization of PPM that allows more than one pulse per symbol interval. Thus, if $\tilde{Q}$ is the PPM alphabet size – i.e., the number of disjoint pulse slots per symbol signaling interval T, and the number of pulses allowed is $\tilde{p}$, the *fixed composition* MPPM codebook is obtained by taking all $\tilde{Q}$-length binary codewords having exactly $\tilde{p}$ coordinates equal to one. The waveform generated by the encoder $\lambda_m(t), 0 \leq t \leq T$ admits the peak-power A whenever the corresponding binary codeword admits the value one and it is zero otherwise. Henceforth we shall refer to this modulation scheme as a $(\tilde{Q}, \tilde{p}, A)$ MPPM scheme.

For a given $\tilde{p}$ the MPPM codebook size equals $\tilde{M} = \binom{\tilde{Q}}{\tilde{p}}$, thus if $\tilde{T}_s$ is the slot duration (pulsewidth) – i.e. $T = \tilde{T}_s \tilde{Q}$, the data rate (in nats/sec) achieved by MPPM is

$$R_{MPPM} = \frac{\ln\left[\binom{\tilde{Q}}{\tilde{p}}\right]}{\tilde{T}_s \tilde{Q}} \quad \text{nats/sec} \ .$$

In an optical direct-detection system the message is transmitted by modulating the intensity $\lambda(t)$ of a photon emitting source. At the same time the receiver records the exact time arrivals of the individual photons that follow a Poisson probability law with an intensity $\lambda(t) + \lambda_0$, where λ_0 denotes the dark current. The capacity of this direct-detection photon channel under peak and average power constraints imposed on $\lambda(t)$ was derived by Kabanov [11], Davis [12] and Wyner [14]. The error exponent and construction of specific codes achieving capacity were also reported in [14], and in particular it was shown that binary signaling is capacity achieving. It should be emphasized, however, that in references [11]-[14] no bandwidth constraints were imposed on $\lambda(t)$.

In [15] Shamai incorporates (in addition to the peak and average power constraints) a bandwidth constraint on $\lambda(t)$ via restricting the minimal time interval Δ in which $\lambda(t)$ must remain constant. A simple piecewise constant pulse amplitude modulated waveform $\lambda(t) = \lambda_i, t \in [(i-1)\Delta, i\Delta]$ satisfying the constraints is considered. The main contribution of Shamai is in showing that the capacity achieving input sequence $\{\lambda_i\}$ is an i.i.d. sequence with a discrete probability mass function having finite support. It is demonstrated in [15] that when Δ is restricted to be larger than a threshold Δ_0, which depends on the dark current intensity λ_0, binary signaling is no longer capacity achieving.

Motivated by the results of Shamai, this work investigates the performance of an extension of MPPM which allows two pulse levels per each "active" signaling slot. Specifically, we consider a fixed composition signaling scheme the symbol interval of which is equal to that of the MPPM symbol

interval T, yet the number of available slots Q is strictly smaller than $\tilde{Q}$. Furthermore, in each symbol; p out of the Q available slots are pulsed, p_1 out of the p pulsed slots are of level A_1 while the rest $p-p_1$ are of level A_2, where $A_2 > A_1$. The fixed composition three-level MPPM codebook is obtained by taking all Q-length ternary codewords having exactly: p_1 coordinates equal to 1; $p-p_1$ coordinates equal to 2; while the rest $Q-p$ equal to 0. In what follows we shall refer to this modulation scheme as a (Q, p, p_1, A_1, A_2) 3L-MPPM scheme.

Given the parameters (Q, p, p_1) the size of this 3L-MPPM codebook equals $M = \binom{Q}{p}\binom{p}{p_1}$, and therefore the data rate achieved by 3L-MPPM, assuming that the slot duration equals T_s (with $T_s Q = T$), is

$$R_{3L-MPPM} = \frac{\ln\left[\binom{Q}{p}\binom{p}{p_1}\right]}{T_s Q} \quad \text{nats/sec} \ .$$

The question is: for a given requirement on data rate and transmitter average-power constraint, how far can this 3L-MPPM scheme compete with MPPM in order to save bandwidth while delivering the same detection quality. Consequently, for a fixed symbol interval T and a given $(\tilde{Q}, \tilde{p}, A)$ MPPM reference scheme our focus will be in analyzing a respective (Q, p, p_1, A_1, A_2) 3L-MPPM scheme for which $Q < \tilde{Q}, M \geq \tilde{M}$, the average-power constraint is the same as that of the $(\tilde{Q}, \tilde{p}, A)$ MPPM scheme, in order to find out whether the symbol error probability in both schemes is comparable if symbol frame synchronizm is implicitly assumed. Even though we impose just the same average-power constraint on both schemes, as we envision a three-level PAM modulation for the extended MPPM scheme the results of Shamai [15] imply that as long as the final peak-power of the 3L-MPPM scheme is finite the capacity achieving distribution for this scenario indeed has a discrete support.

In [13] Frey considered the information capacity of the bandwidth unlimited Poisson channel subject to an encoder time-varying peak constraint $c(t)$ that may be chosen freely subject only to the constraint

$$\frac{1}{T}\int_0^T c(t)dt \leq P \ , \tag{1}$$

for some given $P > 0$. Then, for a known nonrandom noise intensity $\lambda_0(t)$, the channel capacity is found to be $C = P/e$.

In fact, the average-power constraint that we consider in our bandwidth limited 3L-MPPM model falls under the category (1). This, as implied by Frey's result, renders the bandwidth unlimited capacity finite and consequently the capacity for our model is also finite. Asymptotic results regarding the capacity for the model considered herein have recently been reported in [17].

For MPPM in the quantum limited regime an *exact* expression for the symbol error probability is given in [7, Equation (8)]. Thus, in order to compare the detection quality of both schemes a tight upper bound on the symbol error probability for 3L-MPPM in this regime is called for, and this is the first main result in this work. For the noisy channel, a general bound concerning binary hypothesis testing in a direct-detection system is combined with the union bound in [7] to derive an upper bound on the symbol error probability. Following the same arguments we focus here on obtaining an expression for the distance profile of 3L-MPPM in order to compare the corresponding upper bounds in the noisy channel case as well.

The paper is organized as follows. Section II presents the communication model studied here. Section III describes the detection problem precisely and derives the optimum decision rule for our

model. Section IV analyzes the error probability of the optimal receiver for the quantum-limited channel, while the capacity for this case is considered in Section V. In Section VI an expression for the cutoff rate valid for both the noisy and the quantum-limited channel is obtained, while Section VII considers a general upper bound on the error probability for this case. Finally, in section VIII we consider a few specific 3L-MPPM configurations for which we demonstrate the bandwidth efficiency that they offer as compared to MPPM schemes having the same throughput, error probability, and average-power constraint.

II. Communication model

To be explicit, the single-user Poisson channel model studied here is described as follows. The codebook consists of M ternary Q-length codewords. Assuming the encoder wishes to transmit the message $m \in \{1, \ldots, M\}$ it picks the mth codeword $c_m \in \{0,1,2\}^Q$ and generates a 3L-MPPM input $\lambda_m(t)$, $0 \le t \le T$ that satisfies

$$\lambda_m(t) \;=\; \begin{cases} A_1 & t \in [(l-1)T_s, lT_s] \text{ and the } l\text{th component of } c_m \text{ is } 1 \\ A_2 & t \in [(l-1)T_s, lT_s] \text{ and the } l\text{th component of } c_m \text{ is } 2 \\ 0 & t \in [(l-1)T_s, lT_s] \text{ and the } l\text{th component of } c_m \text{ is } 0 \end{cases} ,$$

and

$$T_s\left(p_1 A_1 + (p-p_1)A_2\right) = \tilde{p} A \tilde{T}_s \le \sigma A T \;, \tag{2}$$

where $0 < \sigma < 1$ defines the average-power constraint for both schemes and it is implicitly assumed in (2) that $\tilde{Q}\tilde{T}_s = QT_s = T$.

The waveform $\lambda_m(t)$ determines the rate of a corresponding doubly stochastic Poisson process $d(t)$. Specifically, $d(t)$ corresponds to the number of counts registered by a direct detection device in the interval $[0,t]$, in reaction to the input $\lambda_m(t)$. The observation is

$$\nu(t) = d(t) + D(t) \;,$$

which is also a Poisson process with instantaneous rate $\lambda(t) = \lambda_0 + \lambda_m(t)$. The dark current represented by $D(t)$ is a homogeneous Poisson process of rate λ_0. Thus, conditional on the input $\{\lambda(t)\}$, the signal $\{\nu(t)\}$ is a counting process with independent increments and

$$\Pr\left(\nu(t) - \nu(s) = k | \{\lambda(t)\}\right) = e^{-\int_s^t \lambda(\tau)d\tau} \frac{\left(\int_s^t \lambda(\tau)d\tau\right)^k}{k!} \;,\; t \ge s \;,\; k \in \mathbb{Z}^+ \;. \tag{3}$$

Here $\mathbb{Z}^+$ denotes the set of nonnegative integers.

III. Optimum receiver for constant composition 3L-MPPM

Following the formulation of Lapidoth in [16] a channel use is a pair of probability measures, P^0 and P^m, defined on a measurable space $(\Omega, \mathcal{F})$ on which the "input" process $\lambda(t)$, and the "output" process $\nu(t)$, are defined. The probability measure P^0 serves as a reference probability measure in the sense that $\nu(t)$ is a homogeneous Poisson process of intensity λ_0 with respect to its natural history $\mathcal{F}_t^\nu$ and the measure P^0. We shall use the notation that $\nu(t)$ admits the $(P^0, \mathcal{F}_t^\nu)$-intensity λ_0. It is

further assumed that P^m is absolutely continuous with respect to P^0, i.e., $P^m \ll P^0$, and with respect to the measure P^m the output process $\nu(t)$ admits the predictable $(P^m, \mathcal{F}_t^\nu)$-intensity $\lambda_m(t)$.

Thus, a convenient description of P^m is expressed via its Radon-Nykodim derivative with respect to the reference probability P^0. Denote by P_t^v the restriction of P^v to $\mathcal{F}_t^\nu, v \in \{0, m\}$, and define the $(P^m, \mathcal{F}_t^\nu)$ martingale L_t by

$$L_t = \frac{dP_t^m}{dP_t^0} \ .$$

By [18] it follows that

$$L_t = \left[\prod_{n\geq 1} \frac{\lambda_{T_n}}{\lambda_0} \chi_{\{T_n \leq t\}}\right] \cdot \exp\left\{\int_0^t [\lambda_0 - \lambda_m(s)]\, ds\right\} \ , \tag{4}$$

where T_n denotes the stopping time when the nth jump occurred, and $\chi_{\{G\}}$ denotes the indicator function of the set G.

As the processes $\lambda_m(t), m \in \{1, \ldots, M\}$ defined by our 3L-MPPM construction are all adapted to $\mathcal{F}_t^\nu$, they are $\mathcal{F}_t^\nu$ predictable. The existence of a measure P^m which induces a predictable $\mathcal{F}_t^\nu$-intensity given by $\lambda_m(t)$ follows now by [18].

To this end let the decoder observe $\nu_k = \left\{\nu(t) : t \in T^{(k)} = [(k-1)T, kT]\right\}$ as it is assumed throughout that symbol synchronizm is available for the decoder, and according to (4) a maximum-likelihood decision rule can be defined via the Radon-Nykodim derivative

$$\begin{aligned} L_{T^{(k)}}(\lambda_m, \lambda_{m'}) = \frac{dP_t^m}{dP_t^{m'}} &= \left[\prod_{n\geq 1} \frac{\lambda_{T_n}^m}{\lambda_{T_n}^{m'}} \chi_{\{T_n \leq t\}}\right] \cdot \exp\left\{\int_0^t [\lambda_{m'}(s) - \lambda_m(s)]\, ds\right\} \\ &= \prod_{n\geq 1} \frac{\lambda_{T_n}^m}{\lambda_{T_n}^{m'}} \chi_{\{T_n \leq t\}} \ , \end{aligned} \tag{5}$$

where the last step in (5) follows by the constant composition property of the 3L-MPPM code.

- Let $\{c_i\}, i = 1, \ldots, M$ be the set of all Q-length ternary sequences having p_1 coordinates equal to 1 and $p - p_1$ coordinates equal to 2 (namely the set of messages that could have been transmitted in the form of an 3L-MPPM symbol).

- Let $\boldsymbol{w}_i = \{w_{i_1}, w_{i_2}, \ldots, w_{i_p}\}$ be the set of p distinct integers taking values in the set $\{1, 2, \ldots, Q\}$ indicating the positions of pulsed slots, either with A_1 or A_2 levels, in the ith message.

- Let $\boldsymbol{z}_i = \{z_{i_1}, z_{i_2}, \ldots, z_{i_{p-p_1}}\}$ be the set of $p - p_1$ distinct integers taking values in the set $\{1, 2, \ldots, Q\}$ indicating the positions of A_2 pulsed slots in the ith message.

Noting that the Poisson process $\nu(t), (k-1)T \leq t \leq kT$, during the kth symbol time, is split into Q independent Poisson processes with parameters

$$\int_{(l-1)T_s}^{lT_s} \lambda(t)dt = \begin{cases} (A_1 + \lambda_0)T_s & \text{if slot } l \text{ is pulsed with } A_1 \\ (A_2 + \lambda_0)T_s & \text{if slot } l \text{ is pulsed with } A_2 \\ \lambda_0 T_s & \text{if slot } l \text{ is not pulsed} \end{cases} ,$$

it follows from (5) that the ML decoder collects the sufficient statistics

$$N_l^{(k)} \triangleq \{\text{number of arrivals registered on signaling slot } l \ , \ l \in \{1,\ldots,Q\} \text{ during } k\text{th symbol}\} \ ,$$

and decides upon that message m which maximizes simultaneously, the number of arrivals collected over $\boldsymbol{w}_m$ and the number of arrivals collected over $\boldsymbol{z}_m$, as compared to any $m' \neq m$.
That is,

$$D\left(\nu_0^{T^{(k)}}\right) \ = \ \arg\left\{\max_{1\le m\le M}\left(\sum_{r\in\boldsymbol{w}_m} N_r^{(k)}\right)\bigcap\max_{1\le m\le M}\left(\sum_{j\in\boldsymbol{z}_m} N_j^{(k)}\right)\right\} \ , \tag{6}$$

if such an index exists, while otherwise an erasure is declared. In other words, the decoder accumulates the number of photons in each pulsed slot (either by A_1 or by A_2) for each possible transmitted hypothesis, and additionally it accumulates the number of arrivals in each pulsed A_2 slot. It then declares the message corresponding to the symbol that simultaneously maximizes both results.

In the quantum-limited regime, when $\lambda_0 = 0$ and arrivals can appear only over the p "active" signaling slots, the ML decoding rule (6) simplifies to

$$D\left(\nu_0^{T^{(k)}}\right) = \arg\max_{1\le m\le M}\left(\sum_{j\in\boldsymbol{z}_m} N_j^{(k)}\right) \ , \tag{7}$$

if such an index exists, while otherwise an erasure is declared.

Thus, (6) defines a decoder which is a measurable mapping $D : \mathcal{F}^{\nu}_{T^{(k)}} \to \{1,2,\ldots,M\}\cup\{\text{erasure}\}$, where we allow for the decoder to declare an erasure, and the average probability of error assuming equi-probable messages, P_e, is

$$P_e = 1 - \frac{1}{M}\sum_{i=1}^{M} P^i(D^{-1}(i)) \ . \tag{8}$$

IV. Error probability analysis in the quantum-limited regime

In this section we derive an upper bound on the symbol error probability for 3L-PPM in a quantum-limited channel. Recall that for the reference $(\tilde{Q},\tilde{p},A)$ MPPM scheme the exact expression for the symbol error probability (in the quantum-limited regime) was derived in [7, pp. 1315], namely

$$P_e = \sum_{\ell=1}^{\tilde{p}} \frac{\delta_k - 1}{\delta_k}\binom{\tilde{p}}{k}\epsilon^k(1-\epsilon)^{\tilde{p}-k} \ , \tag{9}$$

where $\delta_k \triangleq \binom{\tilde{Q}-\tilde{p}+k}{k}$, and $\epsilon \triangleq e^{-A\tilde{T}_s}$ is the pulse-erasure probability. An error probability upper bound for 3L-MPPM will provide us with the ability to assess the performance of any (Q,p,p_1,A_1,A_2) scheme in contrast to a reference $(\tilde{Q},\tilde{p},A)$ one.

When 3L-MPPM modulation is used in the quantum-limited regime the decoder (7) errs when either of the following events occurs

1. An active slot has been erased due to lack of arrivals.

2. A misdetection has happened due to an $A_1 \leftrightarrow A_2$ "switch". This happens whenever the number of arrivals over an A_1 slot is at least as large as that over an A_2 slot.

Define $P_{e_1}^m$ and $P_{e_2}^m$ as

$$\begin{aligned} P_{e_1}^m &\triangleq \Pr\{\text{ An active slot has been erased}|m \text{ was sent}\} \\ P_{e_2}^m &\triangleq \Pr\{\text{ A misdetection has happened}|m \text{ was sent}\} \ , \end{aligned}$$

then the union of events bound implies

$$1 - P^m(D^{-1}(m)) \leq P_{e_1}^m + P_{e_2}^m \ . \tag{10}$$

Due to the symmetry of the 3L-MPPM codebook, combining (8) with (10) it follows that

$$P_e = 1 - P^i(D^{-1}(i)) \leq P_{e_1}^i + P_{e_2}^i \ , \tag{11}$$

for an arbitrary transmitted message i.

The probability of error $P_{e_1}^i$ caused by slot erasures is computed as follows.

- When the number of slot erasures ℓ, is not larger than p_1:
  1. If there is at least one A_2 slot erasure among these $\ell \leq p_1$ slot erasures, the decoder will err with probability one.
  2. When all ℓ slot erasures are on A_1 slots, then the decoder takes a random decision among the $\alpha_\ell \triangleq \binom{Q-(p-\ell)}{\ell}$ symbols which admit active pulses (both A_1 and A_2 type) on the $p-\ell$ positions over which arrivals have been registered.
- When the number of slot erasures ℓ, is larger than p_1:
  1. If there is at least one A_1 slot that hasn't been erased the decoder will err with probability one.
  2. When all A_1 slots have been erased together with $\ell - p_1$ additional A_2 slots, the decoder takes a random decision among the $\beta_\ell \triangleq \binom{Q-(p-\ell)}{\ell}\binom{\ell}{p_1}$ symbols which admit active pulses of type A_2 on the $p-\ell$ positions over which arrivals have been registered.

Let $\epsilon_\mu = e^{-A_\mu T_s}, \mu = 1, 2$ be the pulse-erasure probability for an A_μ pulsed slot. The above arguments yield the expression

$$\begin{aligned} P_{e_1}^i \quad = \quad & \sum_{\ell=1}^{p_1} \Bigg\{ \sum_{\ell_1=1}^{\ell-1} \binom{p_1}{\ell_1}\binom{p-p_1}{\ell-\ell_1} \epsilon_1^{\ell_1}(1-\epsilon_1)^{p_1-\ell_1}\epsilon_2^{\ell-\ell_1}(1-\epsilon_2)^{p-p_1-(\ell-\ell_1)} \\ & \qquad + \binom{p_1}{\ell}\frac{\alpha_\ell - 1}{\alpha_\ell}\epsilon_1^{\ell}(1-\epsilon_1)^{p_1-\ell}(1-\epsilon_2)^{p-p_1} \Bigg\} \\ & + \sum_{\ell=p_1+1}^{p} \Bigg\{ \sum_{\ell_1=1}^{p_1-1} \binom{p_1}{\ell_1}\binom{p-p_1}{\ell-\ell_1} \epsilon_1^{\ell_1}(1-\epsilon_1)^{p_1-\ell_1}\epsilon_2^{\ell-\ell_1}(1-\epsilon_2)^{p-p_1-(\ell-\ell_1)} \\ & \qquad + \binom{p-p_1}{\ell-p_1}\epsilon_1^{p_1}\epsilon_2^{\ell-p_1}(1-\epsilon_2)^{p-\ell}\frac{\beta_\ell - 1}{\beta_\ell} \Bigg\} \end{aligned} \tag{12}$$

Suppose that some arbitrary message i was transmitted,

- Let $\boldsymbol{x} = (x_{\imath_1}, x_{\imath_2}, \ldots, x_{\imath_{p_1}})$ be the random vector representing the number of registered arrivals on the p_1 slots $(\imath_1, \imath_2, \ldots, \imath_{p_1})$ where $\lambda_i(t)$ admits the value A_1.
- Let $\boldsymbol{y} = (y_{\jmath_1}, y_{\jmath_2}, \ldots, y_{\jmath_{p-p_1}})$ be the random vector representing the number of registered arrivals on the $p - p_1$ slots $(\jmath_1, \jmath_2, \ldots, \jmath_{p-p_1})$ where $\lambda_i(t)$ admits the value A_2.
- Let the random variables $V_1(i)$ and $V_2(i)$ be defined as

$$\begin{aligned} V_1(i) &\triangleq \min\left\{y_{\jmath_1}, y_{\jmath_2}, \ldots, y_{\jmath_{p-p_1}}\right\} \\ V_2(i) &\triangleq \max\left\{x_{\imath_1}, x_{\imath_2}, \ldots, x_{\imath_{p_1}}\right\} \ . \end{aligned}$$

A misdetection due to an $A_1 \leftrightarrow A_2$ "switch" will happen when the number of arrivals registered on an A_1 slot exceeds that number registered on an A_2 slot. Consequently,

$$\begin{aligned} P_{e_2}^i &\leq \Pr\left\{V_2(i) \geq V_1(i) | \lambda_i(\cdot)\right\} \\ &= 1 - \Pr\left\{V_1(i) - V_2(i) > 0 | \lambda_i(\cdot)\right\} \ , \end{aligned} \tag{13}$$

where the inequality follows by the fact that we count the event $\{V_2(i) = V_1(i)\}$ as an error, and

$$\begin{aligned} \Pr\left\{V_1(i) - V_2(i) > 0 | \lambda_i(\cdot)\right\} &= \sum_{\ell} \Pr\{V_2(i) = \ell\} \Pr\{V_1(i) > \ell\} \\ &= \sum_{\ell} \Pr\{V_1(i) = \ell\} \Pr\{V_2(i) < \ell\} \ . \end{aligned} \tag{14}$$

Since the components of $\boldsymbol{x}$ as well as those of $\boldsymbol{y}$ are independent and identically distributed Poisson r.v.'s with parameters $A_1 T_s$ and $A_2 T_s$ respectively, one can apply results on *order statistics* in order to compute the probability density function of $V_1(i)$ and $V_2(i)$.
To this end let $(v_1, v_2, \ldots, v_{p_1})$ be the ordered version of $(x_{\imath_1}, x_{\imath_2}, \ldots, x_{\imath_{p_1}})$, then following the proof of [19, p. 185] we have

$$\Pr\left\{v_\ell = n\right\} = p_1 \binom{p_1 - 1}{\ell - 1} \Big[\Pr\left\{x \leq n\right\}\Big]^{\ell - 1} \Pr\left\{x = n\right\} \Big[\Pr\left\{x \geq n\right\}\Big]^{p_1 - \ell} \ . \tag{15}$$

Applying (15) for $\ell = p_1$ to obtain the statistics of $V_2(i)$ and then for $\ell = 1$ for $(v_1, v_2, \ldots, v_{p-p_1})$ being the ordered version of $(y_{\jmath_1}, y_{\jmath_2}, \ldots, y_{\jmath_{p-p_1}})$ we conclude that

$$\begin{aligned} \Pr\{V_1(i) = n\} &= (p - p_1)\Big[\Pr\{y \geq n\}\Big]^{p - p_1 - 1} \Pr\{y = n\} \\ \Pr\{V_2(i) = n\} &= p_1\Big[\Pr\{x \leq n\}\Big]^{p_1 - 1} \Pr\{x = n\} \ , \end{aligned} \tag{16}$$

where

$$\begin{aligned} \Pr\{x = n\} &= e^{-A_1 T_s} \frac{(A_1 T_s)^n}{n!} \\ \Pr\{y = n\} &= e^{-A_2 T_s} \frac{(A_2 T_s)^n}{n!} \ . \end{aligned}$$

It can also be verified that

$$\begin{aligned}\Pr\{V_1(i) \leq n\} &= \sum_{\ell=1}^{p-p_1} \binom{p-p_1}{\ell} \Big[\Pr\{y \leq n\}\Big]^{\ell} \Big[\Pr\{y \geq n\}\Big]^{p-p_1-\ell} \\ &= 1 - \Pr\{V_1(i) > n\} \\ \Pr\{V_2(i) \leq n\} &= \Big[\Pr\{x \leq n\}\Big]^{p_1} \ . \end{aligned} \tag{17}$$

The expressions (16)-(17) for the p.m.f's and distribution functions of $V_1(i)$ and $V_2(i)$ can now be used in (14) to provide the sought for upper bound (13) on $P_{e_2}^i$.

In [21] de Caen obtained the following lower bound for the probability of a union of events $\{A_i\}_{i\in\mathcal{I}}$ in a probability space $(\Omega, \mathcal{F}, P)$.

$$P\left(\bigcup_{i\in\mathcal{I}} A_i\right) \geq \sum_{i\in\mathcal{I}} \frac{[P(A_i)]^2}{\sum_{j\in\mathcal{I}} P(A_i \cap A_j)} \ . \tag{18}$$

Particularizing (18) to our case wherein $A_1 = e_1$ and $A_2 = e_2$ one obtains

$$P\left(e_1 \cup e_2\right) \geq \frac{[P(e_1)]^2}{P(e_1) + P(e_1 \cap e_2)} + \frac{[P(e_2)]^2}{P(e_2) + P(e_1 \cap e_2)} \ . \tag{19}$$

Consequently, if $P(e_1 \cap e_2) \ll \max\{P(e_1), P(e_2)\}$ the union of events bound (11) is tight, whereas if $P(e_1) \approx P(e_2)$ the union bound is within a factor of 2 from the exact lower bound on the r.h.s. of (19).

Remark :

The bounding technique presented in this section can be extended to the case where $\lambda_0 > 0$ as follows.

- Define an "erasure" event as the event where the decoder (6) identifies incorrectly the p active slots.
- Define a misdetection event as the event where the decoder (6) identifies correctly the p active slots but then fails to recover the correct message.

Insofar as $\lambda_0 > 0$ suppose that message i was transmitted and let $\boldsymbol{u} = (u_{\ell_1}, u_{\ell_2}, \ldots, u_{\ell_{Q-p}})$ be the random vector representing the number of registered arrivals on the $Q-p$ slots $(\ell_1, \ell_2, \ldots, \ell_{Q-p})$ where $\lambda_i(t) = 0$ and just the dark current is active..

Let the random variables $V_3(i)$ and $V_4(i)$ be defined as

$$\begin{aligned} V_3(i) &\triangleq \min\left\{x_{\imath_1}, x_{\imath_2}, \ldots, x_{\imath_{p_1}}\right\} \\ V_4(i) &\triangleq \max\left\{u_{\ell_1}, u_{\ell_2}, \ldots, u_{\ell_{Q-p}}\right\} \ . \end{aligned}$$

Then the "erasure" event e_1 can be expressed as

$$e_1 = \{V_1(i) \leq V_4(i)\} \bigcup \{V_3(i) \leq V_4(i)\} \ . \tag{20}$$

Furthermore, the misdetection event e_2 can now be expressed in terms of order statistics expressions analogous to those defining the "switch" event in this section except that the relevant p.m.f's are conditioned on the event e_1^c.

Since the calculations involved with this approach are quite tedious we adopt the Chernoff bound in order to compute in section VII an upper bound on the error probability in the case where $\lambda_0 > 0$.

V. Capacity in the quantum limited regime

The 3L-MPPM direct detection quantum limited channel can be modeled as a DMC with $\binom{Q}{p}\binom{p}{p_1}$ inputs and infinite number of outputs. It can be easily verified that the above channel model is symmetric in the sense defined by Gallager in [20, Section 4.5] as follows.

For any input symbol c_i corresponding to the ith row of the transition matrix, the possible outputs are all vectors $(\boldsymbol{x}, \boldsymbol{y}) \in (\mathbb{Z}^+)^p$ with support $\boldsymbol{w}_i = (w_{i_1}, w_{i_2}, \ldots, w_{i_p})$ that defines the set of coordinates where c_i admits the values 1 or 2. The remaining elements of the ith row (which correspond to all vectors $(\boldsymbol{x}, \boldsymbol{y})$ wherein at least one coordinate falls outside the support of $\boldsymbol{w}_i$) are zero, again independently of i. Thus, the rows of the transition matrix are permutations of one another. Turning to the columns of the transition matrix, we can partition the set of columns into subsets, of $p!\binom{Q}{p}$ columns each, cooresponding to outputs with the same realization of registered photons but located on different slot coordinates. Any column which corresponds to a specific realization vector $(\boldsymbol{x}, \boldsymbol{y})$ admits non-zero entries in $\binom{p}{p_1}$ rows. These rows correspond to those input symbols having the support $\boldsymbol{w}_i$ as defined by the $(\boldsymbol{x}, \boldsymbol{y})$ vector. Thus, for each of these subsets of the transition probability matrix, each row is a permutation of each other row and each column is a permutation of each other column. Therefore, the capacity achieving input distribution is the uniform distribution [20, Theorem 4.5.2].

It follows that, the probability of a specific output vector $(\boldsymbol{x}, \boldsymbol{y})$ can be obtained by considering just the $\binom{p}{p_1}$ aforementioned transition probabilities. Moreover, in the process of enumerating all possible output vectors, as one considers those $(\boldsymbol{x}, \boldsymbol{y})$ vectors admitting non-zero values on a specific set of $p-\ell$ coodinates one needs to decide first which corresponding slots are the "active" ones and only then to consider the corresponding $\binom{p}{p_1}$ transition probabilities. Thus, such a set of $(\boldsymbol{x}, \boldsymbol{y})$ vectors admitting non-zero values on a given set of $p-\ell$ coordinates occupies $\binom{Q-p+\ell}{\ell}$ columns in the channel transition matrix.

Consequently,

$$\Pr(\boldsymbol{x}, \boldsymbol{y}) \;\; = \sum_{i \,:\, p((\boldsymbol{x},\boldsymbol{y})|c_i)>0} p\left((\boldsymbol{x}, \boldsymbol{y})|c_i\right) p(c_i) \;\; ,$$

where

$$\left|\{i : p\left((\boldsymbol{x}, \boldsymbol{y})|c_i\right) > 0\}\right| = \binom{p}{p_1} \;\; . \tag{21}$$

As a result, the general expression for the capacity of a DMC

$$C = \max_{p(x)} \sum_{i=1}^{M} \sum_{j=1}^{\infty} p(y_j|x_i) p(x_i) \ln\left(\frac{p(y_j|x_i)}{p(y_j)}\right) \;\; ,$$

can be written in our case as,

$$C_{3L-MPPM} = \ln M - \sum_{K_1=0}^{\infty} \cdots \sum_{K_{p_1}=0}^{\infty} \sum_{L_1=0}^{\infty} \cdots \sum_{L_{p-p_1}=0}^{\infty} \prod_{n=1}^{p_1} \frac{e^{-A_1 T_s}(A_1 T_s)^{K_n}}{K_n!} \prod_{m=1}^{p-p_1} \frac{e^{-A_2 T_s}(A_2 T_s)^{L_m}}{L_m!}$$
$$\cdot \ln \left[\left(\sum_{i \,:\, p((\boldsymbol{x},\boldsymbol{y})|c_i)>0} p\left((\boldsymbol{x},\boldsymbol{y})|c_i\right) \right) / p\left((\boldsymbol{x},\boldsymbol{y})|c_i\right) \right] , \qquad (22)$$

where in (22) $\boldsymbol{x} = (K_1, \ldots, K_{p_1})$ is a p_1-vector of a specific realization on the A_1 pulsed slots, while $\boldsymbol{y} = (L_1, \ldots, L_{p-p_1})$ is a $(p-p_1)$-vector of a specific realization on the A_2 pulsed slots.

VI. Cutoff rate for the background noise channel

The general expression for the cutoff rate derived in [2], for optical channels with observations modeled by (3), is

$$R_0 = -\ln \left\{ \min_{\{q_i\}} \sum_{i=1}^{M} \sum_{j=1}^{M} q_i q_j \exp\left(-\frac{1}{2} d_{ij}^2\right) \right\} \quad \text{nats/cu} , \qquad (23)$$

where q_i is the prior probability for the ith symbol, and

$$d_{ij}^2 = \int_0^T \left[\sqrt{\lambda_i(t) + \lambda_0} - \sqrt{\lambda_j(t) + \lambda_0} \right]^2 dt . \qquad (24)$$

In 3L-MPPM the squared distance (24) decomposes into combinations of the following components

$$D_{10}^2 \triangleq \left[\sqrt{(A_1 + \lambda_0)T_s} - \sqrt{\lambda_0 T_s} \right]^2$$
$$D_{20}^2 \triangleq \left[\sqrt{(A_2 + \lambda_0)T_s} - \sqrt{\lambda_0 T_s} \right]^2$$
$$D_{12}^2 \triangleq \left[\sqrt{(A_1 + \lambda_0)T_s} - \sqrt{(A_2 + \lambda_0)T_s} \right]^2$$

Furthermore, since our code consists of all combinations of ternary sequences having p_1 coordinates equal to 1 and $p-p_1$ coordinates equal to 2 the squared-distance profile is the same for each codeword. As a result we may fix say c_1, and consider all different configurations of $d_{1j}^2, j \neq 1$.

To this end note that any symbol $c_j, j \neq 1$ is defined by its configuration w.r.t. c_1 as follows. Let the set of p_1 coordinates of c_j that equal to 1 be split into three subsets of sizes n_{11}, n_{12} and $p_1 - (n_{11} + n_{12})$ respectively. Here n_{11} denotes the cardinality of the set of coordinates for which $c_j = 1 \cap c_1 = 1$, n_{12} denotes the cardinality of the set of coordinates for which $c_j = 1 \cap c_1 = 2$, while $p_1 - (n_{11} + n_{12})$ denotes the cardinality of the set of coordinates for which $c_j = 1 \cap c_1 = 0$. Similarly, let the set of $p - p_1$ coordinates of c_j that equal to 2 be split into three subsets of sizes n_{21}, n_{22} and $p - p_1 - (n_{21} + n_{22})$ respectively. Here n_{21} denotes the cardinality of the set of coordinates for which $c_j = 2 \cap c_1 = 1$, n_{22} denotes the cardinality of the set of coordinates for which $c_j = 2 \cap c_1 = 2$, while $p - p_1 - (n_{21} + n_{22})$ denotes the cardinality of the set of coordinates for which $c_j = 2 \cap c_1 = 0$.

The restrictions on $(n_{11}, n_{12}, n_{21}, n_{22})$ are

$$\begin{aligned} n_{11} + n_{12} &\leq p_1 \\ n_{21} + n_{22} &\leq p - p_1 \\ n_{11} + n_{21} &\leq p_1 \\ n_{12} + n_{22} &\leq p - p_1 \ . \end{aligned}$$

Any such configuration entails $p_1 - (n_{11} + n_{21})$ coordinates for which $c_j = 0 \cap c_1 = 1$ and $p - p_1 - (n_{12} + n_{22})$ coordinates for which $c_j = 0 \cap c_1 = 2$. As a result, such a configuration corresponds to a squared-distance of

$$d_{1j}^2(n_{11}, n_{12}, n_{21}, n_{22}) = (n_{12} + n_{21}) \left(D_{12}^2 - D_{10}^2 - D_{20}^2 \right) + 2(p_1 - n_{11}) D_{10}^2 + 2(p - p_1 - n_{22}) D_{20}^2 \ .$$

The number of symbols $c_j, j \neq 1$ having such a configuration is

$$\begin{aligned} &L(n_{11}, n_{12}, n_{21}, n_{22}) = \\ &\quad \binom{p_1}{n_{11}} \binom{p_1 - n_{11}}{n_{12}} \binom{p - p_1}{n_{21}} \binom{p - p_1 - n_{21}}{n_{22}} \binom{Q - p}{p_1 - (n_{11} + n_{21})} \binom{Q - p - p_1 + n_{11} + n_{21}}{p - p_1 - (n_{12} + n_{22})} \end{aligned}$$

Following the same arguments as in [7, section II.A] one concludes that the uniform distribution is the minimizing distribution in (23) and consequently

$$R_{0,3L-MPPM} = -\ln \left\{ \frac{1}{M} \sum_{\vec{n}} L(\vec{n}) \exp \left[-\frac{1}{2} d_{ij}^2(\vec{n}) \right] \right\} \quad \text{nats/cu} \ , \tag{25}$$

where we've used the notation $\vec{n} \triangleq (n_{11}, n_{12}, n_{21}, n_{22})$.

VII. Error probability analysis for the background noise channel

Since the considered 3L-MPPM scheme is a constant composition modulation scheme, we may assume that the symbol c_1 was transmitted. For the noisy channel case, the union of events bound implies

$$\begin{aligned} P_e &\leq \Pr \left\{ \bigcup_{j=2}^{M} \{ L_{T^{(k)}}(\lambda_j, \lambda_1) > 1 | c_1 \} \right\} \\ &\leq \sum_{j=2}^{M} \Pr \{ L_{T^{(k)}}(\lambda_j, \lambda_1) > 1 | c_1 \} \ . \end{aligned}$$

To proceed further, we use the Chernoff bound derived in [7, Appendix B] for any direct detection system and then apply it to our case. This bound reads

$$\Pr \{ L_{T^{(k)}}(\lambda_j, \lambda_1) > 1 | c_1 \} \leq \frac{1}{2} \exp \left\{ \int_0^T \left[-s\tilde{\lambda}_j(t) - (1-s)\tilde{\lambda}_1(t) + \tilde{\lambda}_j^s(t) \tilde{\lambda}_1^{1-s}(t) \right] dt \right\} \ ,$$

where $\tilde{\lambda}_j(t) = \lambda_j(t) + \lambda_0$, $1 \leq j \leq M$, and $0 \leq s \leq 1$ is chosen to minimize the right-hand side.

In 3L-MPPM the intensities $\tilde{\lambda}_j(t)$ admit values from the set $\{\lambda_0, A_1+\lambda_0, A_2+\lambda_0\}$, hence the tightest bound is not necessarily achieved for $s = 1/2$. However, for our purposes we take $s = 1/2$ which yields

$$\Pr\left\{L_{T^{(k)}}\left(\lambda_j, \lambda_1\right) > 1 | c_1\right\} \leq \frac{1}{2}\exp\left\{-\frac{1}{2}\int_0^T \left[\sqrt{\tilde{\lambda}_1(t)} - \sqrt{\tilde{\lambda}_j(t)}\right]^2 dt\right\} \ .$$

Next, applying the distance profile results of 3L-MPPM as developed in the previous Section with regard to the cutoff rate, we conclude that

$$P_e \leq \frac{1}{2}\left\{\sum_{\vec{n}} L(\vec{n}) \exp\left[-\frac{1}{2}d_{ij}^2(\vec{n})\right]\right\} \ . \tag{26}$$

VIII. Numerical results

In this section we consider a few specific 3L-MPPM configurations and compare them with corresponding MPPM schemes. In our comparison we consider the detection quality (probability of error) of both schemes as well as the cutoff rate and capacity, subject to a given requirement on the data rate and average transmitted power. The comparison between any pair of schemes is done as follows.

1. The 3L-MPPM pulse width (slot duration) T_s should be strictly larger than that of the MPPM scheme denoted as $\tilde{T}_s$, in an attempt to save bandwidth while maintaining the same error probability as MPPM.

2. Both configurations should have the same average-power

$$\left[p_1 A_1 + (p - p_1)A_2\right] T_s = \tilde{p} A \tilde{T}_s \ . \tag{27}$$

3. The 3L-MPPM codebook size should be at least as large as that of the MPPM

$$M = \binom{Q}{p}\binom{p}{p_1} \geq \binom{\tilde{Q}}{\tilde{p}} = \tilde{M} \ . \tag{28}$$

This requirement implies that

$$R_{3L-MPPM} = \frac{\log_2 M}{QT_s} \geq \frac{\log_2 \tilde{M}}{\tilde{Q}\tilde{T}_s} = R_{MPPM} \ .$$

It can be verified that inequality (28) can be met while insisting on $Q < \tilde{Q}$ and $p < \tilde{p}$, thus a decrease in bandwidth is feasible without penalizing the rate.

In our search the parameters $\left(\tilde{Q}, \tilde{p}, A, \tilde{T}_s\right)$ of MPPM and (Q, p, p_1) of 3L-MPPM were chosen to satisfy (28), then the parameters (T_s, A_1, A_2) of the 3L-MPPM have been determined to satisfy (27).

Table 1. shows the bandwidth efficiency reduction factor $\beta = Q/\tilde{Q}$ achievable by 3L-MPPM for a few MPPM configurations $\left(\tilde{Q}, \tilde{p}\right)$.

$\tilde{Q}$	$\tilde{p}$	Q	p	p_1	$\frac{M}{\tilde{M}}$	$\beta = \frac{Q}{\tilde{Q}}$
6	3	5	2	1	1.0000	0.8333
8	4	7	3	2	1.5000	0.8750
9	4	8	3	2	1.3333	0.8889
10	5	8	4	2	1.6667	0.8000
10	5	9	3	2	1.0	0.9000
11	5	9	4	2	1.6364	0.8182
12	6	9	5	3	1.3636	0.7500
13	6	10	5	3	1.4685	0.7692
14	7	10	6	3	1.2238	0.7143
15	7	11	6	3	1.4359	0.7333
16	7	12	6	3	1.6154	0.7500
17	8	12	7	4	1.1403	0.7059
18	7	13	6	3	1.0784	0.7222
19	7	14	6	3	1.1920	0.7368
20	9	14	8	4	1.2515	0.7000
21	8	15	7	4	1.1068	0.7143
22	11	15	10	5	1.0728	0.6818
23	9	16	8	4	1.1024	0.6957
24	9	17	8	4	1.3015	0.7083
25	11	17	10	5	1.0995	0.6800
26	10	18	9	5	1.1533	0.6923
27	9	19	8	4	1.1289	0.7037
28	11	19	10	5	1.0841	0.6786
29	10	20	9	5	1.0566	0.6897
30	10	21	9	5	1.2327	0.7000

Table 1: Bandwidth reduction factor of 3L-MPPM over MPPM

Another quantity of practical interest is the peak-to-average ratio α, which for 3L-MPPM is given by $\alpha = A_2 Q / [p_1 A_1 + (p - p_1) A_2]$ as compared to $\alpha = \tilde{Q}/\tilde{p}$ for the MPPM scheme.

In what follows we provide some numerical results for both schemes under the constraints as defined above, wherein it is assumed throughout that $\tilde{T}_s = 1$.

A: Error Probability

Taking as a reference an MPPM scheme with $\tilde{Q} = 10$ and $\tilde{p} = 5$, we examine the performance of a 3L-MPPM scheme with parameters $Q = 9$, $p = 3$ and $p_1 = 2$ in terms of error probability, both in the quantum limited and the background noise regimes.

For the quantum limited channel we choose $A = 8$ for the reference MPPM scheme. Figure 1 illustrates the error probability of 3L-MPPM as a function of A_1, where A_2 is determined according to the average-power requirement (27). It is noticed that an optimal ratio A_2/A_1 exists which achieves a minimum in the error probability. This Figure also illustrates the Chernoff bound, in the quantum limited regime, for this particular case.

Figure 2 shows the two components composing the error probability in Figure 1, namely the slot erasures component $P_{e_1}^i$ and the misdetection component $P_{e_2}^i$, respectively. It is seen that erasure caused detection errors are the dominating factor for large A_2/A_1, while misdetection (switch) errors become the dominating factor when the A_2 and A_1 values are close.

Figure 3 shows the upper bound on P_e against the lower bound implied by de Caen's bound.

Figures 4, 5 and 6 show the Chernoff upper bound on the error probability of 3L-MPPM, in the presence of background noise, for different combinations of reference MPPM scheme and corresponding 3L-MPPM scheme and for various values of λ_0.

B: Cutoff Rate

We compute next the cutoff rate of 3L-MPPM in both regimes : the quantum limited and background noise.

In our search for the optimal parameters of the 3L-MPPM configuration (Q, p, p_1), we maintain the same average power as compared to the corresponding $(\tilde{Q}, \tilde{p}, \tilde{A})$ MPPM reference scheme while allowing the ratio A_2/A_1 to vary.

In the quantum limited case, it is obvious from Table 3 that 3L-MPPM provides better throughput efficiency (in nats/photon) as compared to MPPM. Furthermore, 3L-MPPM becomes more effective and its advantage over MPPM is pronounced further when the symbol is restricted to have relatively low energy.

Table 2 summarizes the cutoff rate results for the background noise channel.

λ_0	A	$\tilde{Q}$	$\tilde{p}$	$R_{0,\text{MPPM}}$	Q	p	p_1	$R_{0,\text{3L-MPPM}}$	$\frac{A_2}{A_1}^*$
1	2	6	3	0.7393	5	2	1	1.303	$\gg 1$
1	4	6	3	1.7758	5	2	1	1.9943	2.4129
1	2	10	5	1.2403	9	3	2	2.1886	6.9108
2	2	10	5	0.8170	9	3	2	2.0430	$\gg 1$
5	10	10	5	4.3605	9	3	2	4.9680	2.2452
10	10	10	5	3.2953	9	3	2	4.3364	2.05040
1	2	11	5	1.3549	9	4	2	2.2461	$\gg 1$

Table 2: 3L-MPPM and MPPM Cutoff rate in the background noise regime

It is seen from Table 2 that 3L-MPPM becomes more effective in the presence of background noise, especially for moderate signal to noise ratios (SNRs). This improvement is due to the flexibility that 3L-MPPM has in choosing the optimal ratio A_2/A_1 subject to the same average power constraint.

C: Capacity in the Quantum-limited Regime

The Capacity of a specific 3L-MPPM scheme in the quantum limited regime is computed using a computer program. For ease of computation we assume that the number of photons detected at each "active" slot admits values in the range $[0, JA_2T_s]$, where $A_2 > A_1$ and J is a parameter (chosen such that the numerical error in the capacity computation is negligible). In this case, the number of possible channel output signals is $L = (JA_2T_s)^p$.

The computation of $\Pr(\boldsymbol{x}, \boldsymbol{y})$ involves the following steps:

- Generation and numbering of the M channel inputs (codewords).
- Generating the transition probabilities $\{p((\boldsymbol{x}_k, \boldsymbol{y}_k)|c_i),\ k = 1, 2, \cdots, L\}$ given a specific input symbol c_i, in a vector of length $L = (JA_2T_s)^p$. This vector will be indexed using a proper index set $I = \{\imath_1, \cdots, \imath_p\}$ according to some predefined rule.
- The index set I_k is derived for each output vector $(\boldsymbol{x}_k, \boldsymbol{y}_k)$.
- Generating the appropriate $\binom{p}{p_1}$ permutations of I_k, creating a group of index sets that would be used to calculate the entries to the transition probability vector.

A comparison between the capacity and cutoff rate of MPPM and 3L-MPPM in the quantum limited regime is given in Table 3. Here the ratio A_2/A_1 for the 3L-MPPM was determined to achieve the highest capacity.

MPPM						3L-MPPM							
A	$\tilde{Q}$	$\tilde{p}$	$r\tilde{T}_s$	R_0	C	Q	p	p_1	rT_s	R_0	C	$\frac{A_2}{A_1}^*$ for R_0	$\frac{A_2}{A_1}^*$ for C
3	6	3	0.4993	2.61	2.792	5	2	1	0.599	2.493	2.70	3.189	3.17
5	6	3	0.4993	2.936	2.968	5	2	1	0.599	2.824	2.912	3.496	3.464
6	6	3	0.4993	2.974	2.985	5	2	1	0.599	2.898	2.950	3.587	3.687
2	10	5	0.5529	3.662	4.409	9	3	2	0.614	4.025	4.69	2.712	3
3	10	5	0.5529	4.611	5.096	9	3	2	0.614	4.748	5.174	3.075	3.19
4	10	5	0.5529	5.129	5.367	9	3	2	0.614	5.145	5.377	3.31	3.625

Table 3: Cutoff rate and Capacity of 3L-MPPM as compared to MPPM. Quantum limited channel.

References

[1] J. R. Pierce, "Optical channels: Practical limits with photon counting," *IEEE Trans. Commun.,* vol. COM-26, No. 12 pp. 1819-1821, December 1978.

[2] D. L. Snyder and I. B. Rhodes, "Some implications of the cutoff rate criterion for coded direct-detection optical communications systems," *IEEE Trans. Inform. Theory,* vol. IT-26, No. 4 pp. 327-338, July 1981.

[3] G. M. Lee and G. W. Schroeder, "Optical pulse-position modulation with multiple positions per pulsewidth," *IEEE Trans. Commun.,* vol. COM-25, No. 3 pp. 360-364, March 1977.

[4] I. Bar-David and G. Kaplan, "Information rates of photon limited overlapping pulse position modulation channels," *IEEE Trans. Inform. Theory,* vol. IT-30, No. 3 pp. 455-464, May 1984.

[5] C. N. Georghiades, "Some implications of TCM for optical direct-detection channels," *IEEE Trans. Commun.,* vol. COM-37, No. 5 pp. 481-487, May 1989.

[6] C. N. Georghiades and J. K. Crutcher, "Throughput efficiency considerations for opticalOPPM," in *Proc. Global Teleommun. Conf.,* (Phoenix, AZ), pp. 430-433, November 1991.

[7] C. N. Georghiades, "Modulation and coding for throughput-efficient optical systems," *IEEE Trans. Inform. Theory,* vol. IT-40, No. 5 pp. 1313-1326, Sep. 1994.

[8] H. M. H. Shalaby, "Performance of uncoded overlapping PPM under communications constraints," in *Proc. Int. Conf. Commun.,* (Geneva, Switzerland), pp. 512-516, May 1993.

[9] H. Sugiyama and K. Nosu, "MPPM : A method of improving the band-utilization efficiency in optical PPM," *J. Lightwave Technol.,* vol. 7, No. 3, March 1989.

[10] James M. Budinger, Mark Vanderaar, P. Wagner and Steven Bibyk, "Combinatorial pulse position modulation for power efficient free-space laser communications," *SPIE Proc.,* vol. 1866, Jan. 1993.

[11] Y. M. Kabanov, "The capacity of a channel of a Poisson type," *Theory Prob. Appl.,* vol. 23, pp. 143-147, 1978.

[12] M. H. A. Davis, "Capacity and cut-off rate for Poisson-type channels," *IEEE Trans. Inform. Theory,* vol. IT-26, No. 6, pp. 710-715, November 1980.

[13] M. R. Frey, "Information capacity of the Poisson channel," *IEEE Trans. Inform. Theory,* vol. IT-37, No. 2, pp. 244-256, March 1991.

[14] A. D. Wyner, "Capacity and error exponent for the direct detection photon channel – parts I and II," *IEEE Trans. Inform. Theory,* vol. IT-34, No. 6 pp. 1449-1471, November 1988.

[15] S. Shamai (Shitz), "Capacity of a pulse amplitude modulated direct detection photon channel," *IEE Proc.,* vol. 137, Pt. I, No. 6 pp. 424-430, Dec. 1990.

[16] A. Lapidoth, "On the reliability function of the ideal Poisson channel with noiseless feedback," *IEEE Trans. Inform. Theory,* vol. IT-39, No. 2, pp. 491-503, March 1993.

[17] A. Lapidoth and S. M. Moser, "The asymptotic capacity of the discrete-time Poisson channel," Winter school on coding and information theory, Monte Verità, Switzerland, Feb. 24-27, 2003.

[18] P. Brémaud, *Point Processes and Queues: Martingale Dynamics.* New-York: Springer-Verlag, 1981.

[19] A. Papoulis, *Probability, Random Variables, and Stochastic Processes.* 3rd ed. New-York: McGraw-Hill, 1991.

[20] R. G. Gallager, *Information Theory and Reliable Communication.* New-York: Wiley, 1968.

[21] D. de Caen, "A lower bound on the probability of a union," *Discr. Math.,* vol. 169, pp. 217-220, 1997.

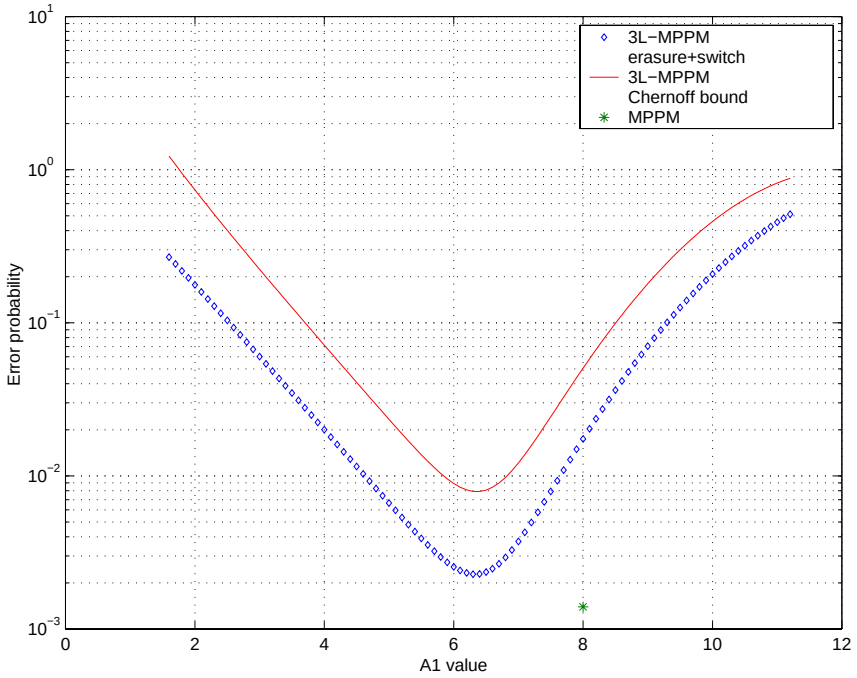

Figure 1: 3L-MPPM error probability as a function of A_1. Quantum limited channel. MPPM parameters $(A = 8, \tilde{Q} = 10, \tilde{p} = 5)$, 3L-MPPM parameters $(Q = 9, p = 3, p_1 = 2)$.

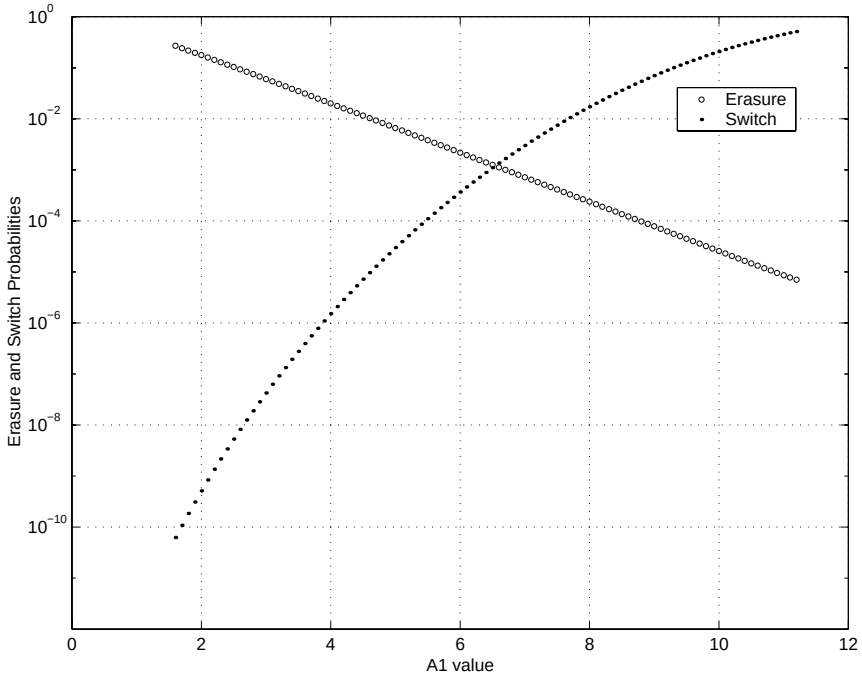

Figure 2: 3L-MPPM erasure and switch probability as a function of A_1. Quantum limited channel. MPPM parameters $(A = 8, \tilde{Q} = 10, \tilde{p} = 5)$, 3L-MPPM parameters $(Q = 9, p = 3, p_1 = 2)$.

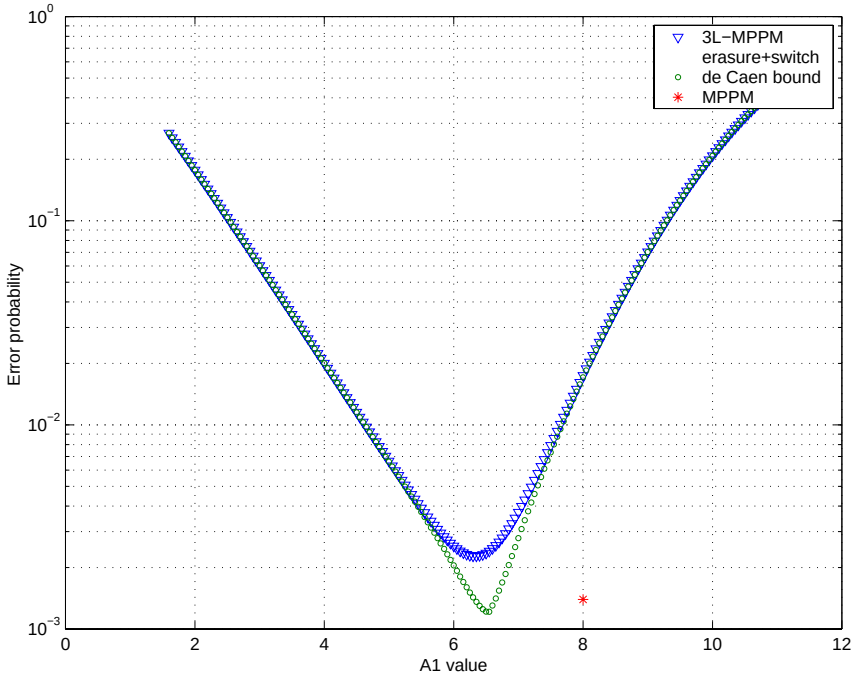

Figure 3: 3L-MPPM error probability vs de Caen bound. Quantum limited channel. MPPM parameters $(A = 8, \tilde{Q} = 10, \tilde{p} = 5)$, 3L-MPPM parameters $(Q = 9, p = 3, p_1 = 2)$.

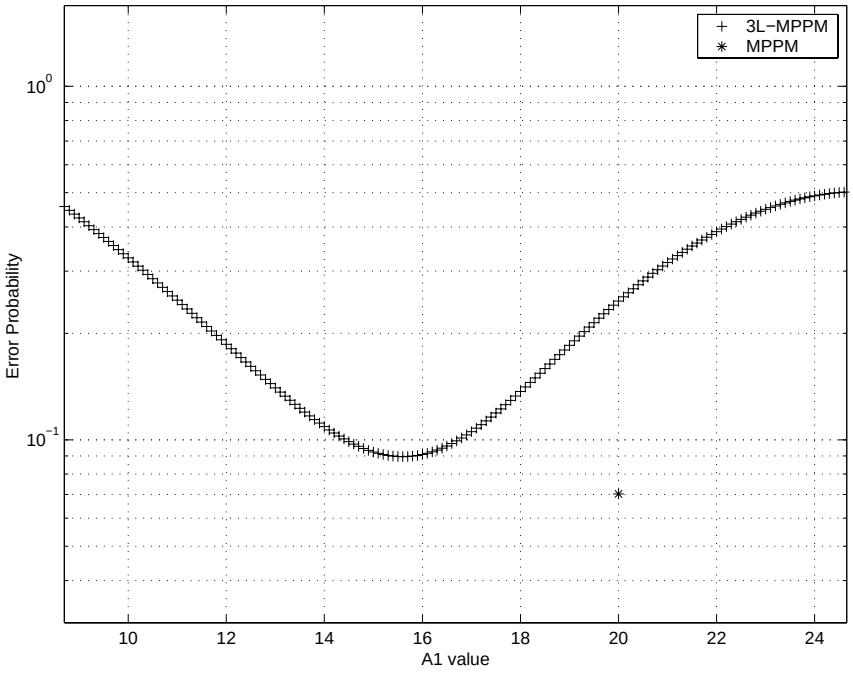

Figure 4: 3L-MPPM error probability upper bound with noise intensity $\lambda_0 = 15$. MPPM parameters $(A = 20, \tilde{Q} = 6, \tilde{p} = 3)$, 3L-MPPM parameters $(Q = 5, p = 2, p_1 = 1)$.

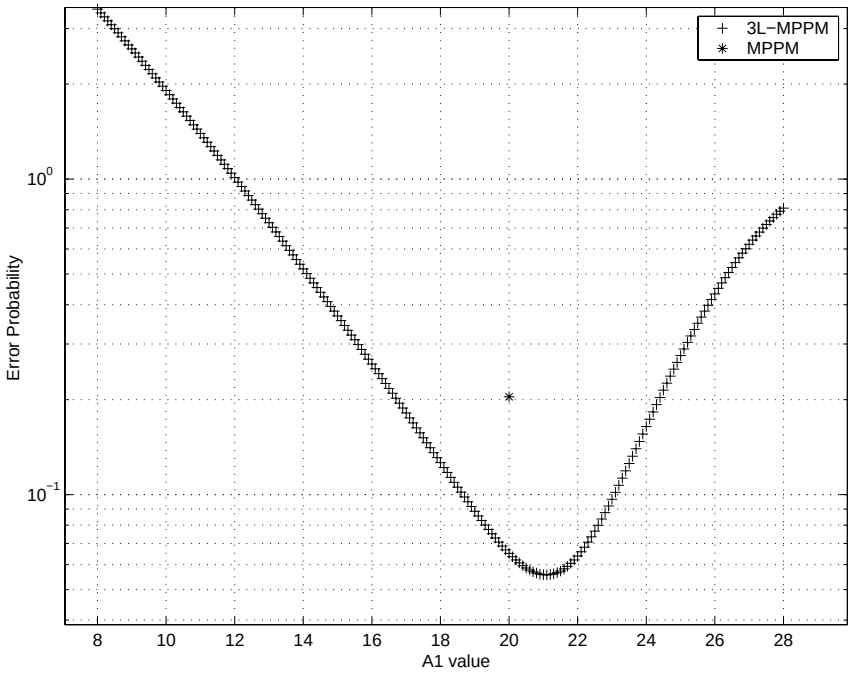

Figure 5: 3L-MPPM error probability upper bound with noise intensity $\lambda_0 = 15$. MPPM parameters $(A = 20, \tilde{Q} = 10, \tilde{p} = 5)$, 3L-MPPM parameters $(Q = 9, p = 3, p_1 = 2)$.

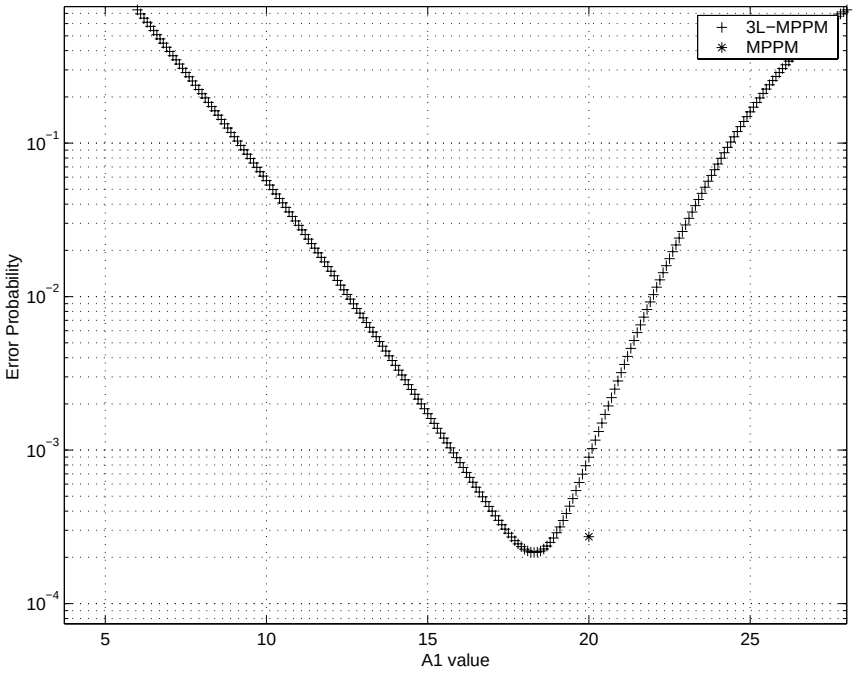

Figure 6: 3L-MPPM error probability upper bound with noise intensity $\lambda_0 = 2$. MPPM parameters $(A = 20, \tilde{Q} = 10, \tilde{p} = 5)$, 3L-MPPM parameters $(Q = 9, p = 3, p_1 = 2)$.